OPEN ACCESS
IOP Publishing
Journal of Physics: Condensed Matter
J. Phys.: Condens. Matter **31** (2019) 505602 (9pp)
https://doi.org/10.1088/1361-648X/ab41b5

Local entanglement and string order parameter in dimerized models

Murod S Bahovadinov[1,2], Oğuz Gülseren[1] and Jürgen Schnack[2]

[1] Department of Physics, Bilkent University, 06800, Bilkent, Ankara, Turkey
[2] Fakultät für Physik, Universität Bielefeld, D-33501 Bielefeld, Germany

E-mail: murodbahovadinov@bilkent.edu.tr

Received 18 June 2019, revised 19 August 2019
Accepted for publication 5 September 2019
Published 27 September 2019

Abstract

In this letter, we propose an application of string order parameter (SOP), commonly used in quantum spin systems, to identify symmetry-protected topological phase (SPT) in fermionic systems in the example of the dimerized fermionic chain. As a generalized form of dimerized model, we consider a one-dimensional spin-1/2 *XX* model with alternating spin couplings. We employ Jordan–Wigner fermionization to map this model to the spinless Su–Schrieffer–Heeger fermionic model (SSH) with generalized hopping signs. We demonstrate a phase transition between a trivial insulating phase and the Haldane phase by the exact analytical evaluation of reconstructed SOPs which are represented as determinants of Toeplitz matrices with the given generating functions. To get more insight into the topological quantum phase transition (tQPT) and microscopic correlations, we study the pairwise concurrence as a local entanglement measure of the model. We show that the first derivative of the concurrence has a non-analytic behaviour in the vicinity of the tQPT, like in the second order trivial QPTs.

Keywords: string order parameter, symmetry protected topological phase, Jordan Wigner fermionization, SSH model, local entanglement, quantum phase transitions

(Some figures may appear in colour only in the online journal)

1. Introduction

A detailed study of the phases of matter and also the transition between them have long been an actual problem of condensed matter physics. While Landau–Ginzburg theory can provide such understanding and explain trivial quantum phase transitions in terms of *'spontaneous symmetry-breaking'*, topological phases of matter and their transitions can not be characterized in the frame of the theory. Particularly, this is due to the lack of a local order parameter that can identify a topological phase. Consequently, exploration of these non-trivial quantum phases and their transitions has been an actively studied topic in the field of condensed matter physics.

The oldest example of a *symmetry-protected topological* (SPT) phase of 1D quantum spin systems is the Haldane phase, which is the ground state phase of the standard antiferromagnetic Heisenberg model with $S = 1$. The gaped nature of the ground state phase and the existence of the edge states were predicted a long time ago [1–3], while no local order was identified to characterize the phase. Later on, Den Nijs and Rommelse [4] have shown that the Haldane phase has a hidden Neel order, which can be identified by the non-local string order parameter (SOP). Kennedy and Tasaki [5] explained the origin of the gap in terms of the hidden $\mathbb{Z}_2 \times \mathbb{Z}_2$ symmetry breaking using non-local unitary transformation. This transformation usually converts SOPs to a simple ferromagnetic order parameter shedding light on the symmetry structure which is protecting the Haldane phase. As a result, for a long

time the only condition for existence of the Haldane phase in spin systems was a non-zero value of SOP. Employing this, in the early 1990s the Haldane phase was detected in modified Heisenberg spin chains with $S = 1$ and Heisenberg ladders with $S = \frac{1}{2}$ both numerically and analytically [6, 7]. In particular, the Haldane phase of the bond-alternating Heisenberg model was also studied numerically using SOP via exact diagonalization methods [8, 9].

While the Haldane phase was identified via SOPs in spin systems, in fermionic and bosonic systems rigorous and generalized tools such as the Berry phase have been used. As a result, the question of generalization of fermionic order parameters for spin systems has arisen. Hastugai *et al* [10] introduced a local spin twist as a generic parameter of Berry phase for gapped spin systems, which has been used extensively [11]. Along this line of thought, Rosch and Anfuso [12] considered the reverse process, i.e. using SOP as an SPT order parameter for fermionic systems. They reconstructed SOP for identification of the SPT phase in band insulators and studied the robustness of the SOP against perturbation terms [13]. More recently, SOP was used to identify the Haldane phase in a 1D bosonic lattice, a topological Kondo insulator and a Kitaev Ladder [14–16], demonstrating their solid application for non-spin systems. However, these works were performed numerically using DMRG [17, 18] and SOPs were not evaluated analytically. As the first result of the present paper, we analytically evaluate SOP to identify the SPT phase in the example of a dimerized fermionic model. The current well-studied model is considered due to it's simplicity and it can demonstrate clearly the physical picture of SOPs. This result, particularly, expands the list of exactly calculable order parameters of SPT phases.

Another question which we address in this letter is the behaviour of local two-site entanglement in the vicinity of topological quantum phase transitions (tQPT). There have been numerous studies carried out on the characterization of topological phases and their transitions in which entanglement entropy and entanglement spectrum are introduced to identify tQPT [19–21] and the corresponding phases. However, only a few studies were carried on the behaviour of local pairwise entanglement in tQPTs [22]. A good measure of local bipartite entanglement is concurrence, defined by Wootters [23], and it has been used extensively to study trivial QPT occuring in 1D quantum spin chains [24–29]. In particular, in [30] it was shown, that in trivial QPT non-analytic behaviour of the concurrence or its derivative determine the order of the quantum transition. Hence, an interesting question to investigate is the behaviour of microscopic correlations and the concurrence in the vicinity of tQPT, which we discussed in the second part of the paper.

The paper is organized as follows. In section 2, we introduce the considered spin model and describe basic steps of fermionization and exact analytical diagonalization of it. Fermionized versions of the SOPs, their exact evaluation and the final phase diagram are presented in section 3. We discuss the behaviour of local bipartite entanglement in the vicinity of topological QPT in section 4. Finally, conclusive notes and future outlooks are presented in the last section section 5.

2. Model definition

We consider a generalized spin-1/2 *XX* chain of length N with bond-alternation defined as:

$$H_1 = J\sum_{i=1}^{N}(S^y_{2i-1}S^y_{2i} + S^x_{2i-1}S^x_{2i}) \tag{1}$$

$$H_2 = J'\sum_{i=1}^{N}(S^y_{2i}S^y_{2i+1} + S^x_{2i}S^x_{2i+1}) \tag{2}$$

where J, J' are spin couplings. The sum of these two terms defines the Hamiltonian of our model:

$$H = H_1 + H_2. \tag{3}$$

We note that J, J' can be ferromagnetic (FM) and antiferromagnetic (AFM) . Since the relative absolute value of couplings define ground state phases of (3), we parameterize $J = 2\cos(\theta)$ and $J' = 2\sin(\theta)$, where $\theta \in [0, 2\pi)$.

Due to broken translational symmetry, one can relabel spins within the effective unit cell and rewrite equations (1) and (2) in the following form:

$$H_1 = \cos(\theta)\sum_{i=1}^{\frac{N}{2}}(S_i^{+(a)}S_i^{-(b)} + S_i^{-(a)}S_i^{+(b)}) \tag{4}$$

$$H_2 = \sin(\theta)\sum_{i=1}^{\frac{N}{2}-1}(S_i^{+(b)}S_{i+1}^{-(a)} + S_i^{-(b)}S_{i+1}^{+(a)}) \tag{5}$$

where (a) and (b) refer to spins located within the ith unit cell. For $\theta = \frac{n\pi}{2}$, $n \in \mathbb{Z}$ one has localized spin dimers along the chain . Hereafter, we assume periodic boundary conditions (PBC).

To fermionize (4) and (5), we use the Jordan–Wigner transformation [31] which we define as:

$$S_i^{+(a)} = a_i^\dagger e^{i\pi\sum_{m<i}(a_m^\dagger a_m + b_m^\dagger b_m)} \tag{6}$$

$$S_i^{+(b)} = b_i^\dagger e^{i\pi\sum_{k<i}(a_k^\dagger a_k + b_k^\dagger b_k + a_i^\dagger a_i)} \tag{7}$$

$$S_i^{z(a)} = a_i^\dagger a_i - 1/2 \tag{8}$$

where operators a_i, b_i are spinless fermionic operators with standard anticommutation rules. This transformation maps (3) to the following fermionic model:

$$\mathcal{H} = \sum_{i=1}^{N_c}\cos(\theta)(a_i^\dagger b_i + b_i^\dagger a_i) + \sin(\theta)(b_i^\dagger a_{i+1} + a_{i+1}^\dagger b_i) \tag{9}$$

where N_c is the number of effective unit cells. In derivation of (9), we neglected boundary terms, assuming that the chain is long enough, so that the boundary terms' contribution to the physical quantities $\sim O(\frac{1}{N})$ is negligible.

The Hamiltonian (9) is a generalized non-interacting Su–Schrieffer–Heeger (SSH) model. It should be noted, that in contrast to the well-studied standard SSH model [32, 33], here one may have different signs of the fermionic hopping parameters (due to the freedom of the signs for spin couplings). Furthermore, if the isotropic Dzyaloshinskiy–Moriya interaction along the chain $H_{\rm DM} = D^z \sum_{i=1}^{L} (S_i^x S_{i+1}^y - S_i^y S_{i+1}^x)$ is introduced to the model (3), one may have complex values of the hoping couplings J, J'. This representation freedom of spin chains in terms of fermions enriches the physical phenomena and may correspond to fictitious fermionic models.

To express (9) in k-space, we use the discrete Fourier transformation of the form:

$$a_j = \frac{1}{\sqrt{N_c}} \sum_{k\in BZ} \mathrm{e}^{-\mathrm{i}kj} a_k, \tag{10}$$

$$b_j = \frac{1}{\sqrt{N_c}} \sum_{k\in BZ} \mathrm{e}^{-\mathrm{i}kj} b_k. \tag{11}$$

Then, the Hamiltonian (9) in the momentum space can be written as:

$$\mathcal{H} = \sum_{k\in BZ} \Gamma_k^\dagger \hat{F}_k \Gamma_k, \tag{12}$$

where

$$\hat{F}_k = \begin{bmatrix} 0 & \mathrm{e}^{-\mathrm{i}\frac{k}{2}} \sin(\theta) + \mathrm{e}^{\mathrm{i}\frac{k}{2}} \cos(\theta) \\ \sin(\theta)\mathrm{e}^{\mathrm{i}\frac{k}{2}} + \mathrm{e}^{-\mathrm{i}\frac{k}{2}} \cos(\theta) & 0 \end{bmatrix} \tag{13}$$

and $\Gamma_k^\dagger = (a_k^\dagger, b_k^\dagger)$. One may get spectrum of the Bogolyubov quasiparticles by diagonalization of the kernel (12),

$$\mathcal{H} = \sum_{k\in BZ} \Psi_k^\dagger \hat{\Lambda}_k \Psi_k, \tag{14}$$

with $\Psi_k^\dagger = (\alpha_k^\dagger, \beta_k^\dagger)$. The matrix elements of the new diagonal kernel Λ_k define the spectrum of the quasiparticles:

$$E^\pm(k,\theta) = \pm\sqrt{1 + \sin(2\theta)\cos(k)}. \tag{15}$$

The vector Ψ_k of qusiparticle operators is connected to the vector Γ_k via,

$$\Psi_k = \hat{U}_k \Gamma_k \tag{16}$$

where $\hat{U}_k$ is the transformation matrix formed out by the eigenvectors,

$$v^\pm = \frac{1}{\sqrt{2}} \begin{pmatrix} \pm\frac{E^+(k,\theta)}{\mathrm{e}^{\mathrm{i}\frac{k}{2}} \sin(\theta) + \mathrm{e}^{-\mathrm{i}\frac{k}{2}} \cos(\theta)} \\ 1 \end{pmatrix}. \tag{17}$$

In figure 1, we plot the spectrum of the quasiparticles for different values of intracell and intercell couplings. For $\theta = 0$ the intercell coupling vanishes, thus one has localised fermions within the unit cell. This flattens the quisiparticle bands, making them have infinite mass. This character in fact is preserved for any $\theta = \frac{n\pi}{2}$, $n \in \mathbb{Z}$.

For other values of the couplings, the bands get dispersed with a finite density of states (DOS). Due to the freedom on couplings' signs, there are two different modes for the system: couplings with the same signs (FM-FM and AFM-AFM, red sectors in figure 1(b)) and couplings with alternating signs (AFM-FM and FM-AFM, blue sectors in figure 1(b)).

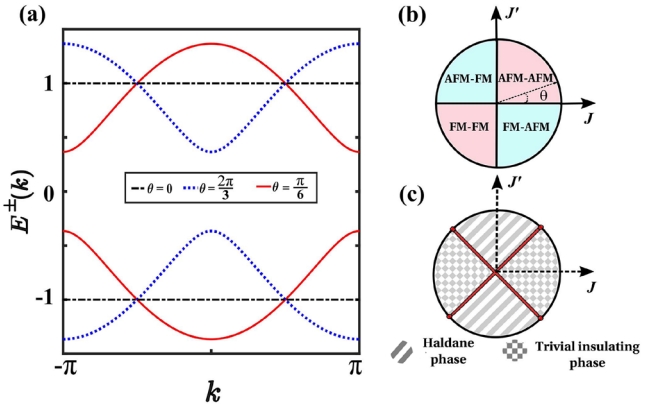

Figure 1. (a) Quasiparticle energy spectra $E^\pm(k,\theta)$ for the values of $\theta = [0, \frac{\pi}{6}, \frac{2\pi}{3}]$. Flat band corresponds to the dimers localized within the unit cell. Remaining dispersive bands represent two modes of the model, as shown in (b). In (c) the phase diagram of the model is shown.

The first mode (red sectors of the unitary circle) has a particle—hole symmetric excitation spectrum with the minimum gap at $k = \pm\pi$, as shown in figure 1(a) (for $\theta = \frac{\pi}{6}$). The value of the gap at $k = \pm\pi$ is

$$\Delta_{G1}(k = \pm\pi) = 2\sqrt{1 - \sin(2\theta)}. \tag{18}$$

These red sectors correspond to the SSH limit, since both couplings have the same signs. In the second mode, which corresponds to the blue sectors of the unitary circle, the intercell (intracell) coupling is ferromagnetic, while intracell (intercell) is antiferromagnetic. Then minimum value of the gap is reached at $k = 0$ and can be determined as,

$$\Delta_{G2}(k = 0) = 2\sqrt{1 + \sin(2\theta)}. \tag{19}$$

From the last expressions (18) and (19) for the gap value, on can see that there are gap closures which occure for $\theta = \frac{(2n+1)\pi}{4}$, $n \in \mathbb{Z}$. These gap closures hint for a quantum phase transition, which happens to have topological nature.

3. Fermionized string order parameters

Previously, the tQPT of the model in the Heisenberg limit was studied via DMRG using SOP and symmetry fractionalization technique [34, 35]. In this section, we show an exact calculation of SOP employing the fermionization approach for our XX model.

For the generalized model (3) the SOP can be defined as [8, 9],

$$O^{S(\gamma)} = \lim_{r\to\infty} O^\gamma(r) \tag{20}$$

$$O^\gamma_{l,m}(r) = -4 \left\langle S_l^{\gamma(b)} \mathrm{e}^{\mathrm{i}\pi(S_{l+1}^{\gamma(a)} + S_{l+2}^{\gamma(b)} + \cdots + S_{m-1}^{\gamma(b)})} S_m^{\gamma(a)} \right\rangle \tag{21}$$

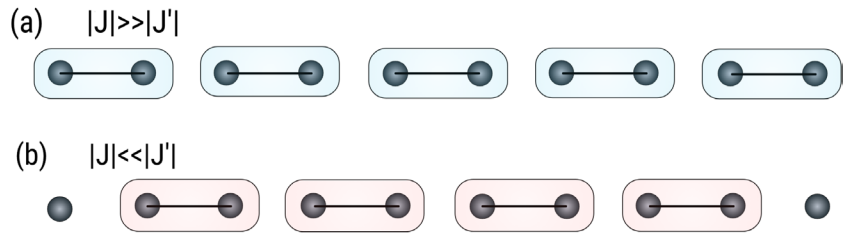

Figure 2. Schematic representation of the maximally entangled pairs formed in the (a) trivial insulating phase ($|J| \gg |J'|$) and (b) in the Haldane phase ($|J| \ll |J'|$). For the chain with OBC in the Haldane phase with $|J| \ll |J'|$ one has free spins at the edges, forming corresponding degenerate edge states which are peculiar to the SPT phases.

where $r = |m - l|$ and $\gamma \in [x, y, z]$. For convenience, we further call (21) *long-range string* (LRS). From equation (20) it is clear that a long-distant limit of LRS defines SOP. Here, the prefactor -4 is used to normalize, so that in the dimerized topological limit $\theta = \frac{(2n+1)\pi}{2}$ it yields $O^{\gamma}_{l,m} = 1$.

For longitudinal LRS, using $\frac{e^{i\pi S^z}}{2i} = S^z$, equation (20) can be written as:

$$O^{z}_{l,m} = \left\langle e^{i\pi(S^{z(b)}_{l} + S^{z(a)}_{l+1} + S^{z(b)}_{l+2} + \cdots + S^{z(b)}_{m-1} + S^{z(a)}_{m})} \right\rangle . \tag{22}$$

Since the model is isotropic, $O^{x}_{l,m} = O^{y}_{l,m}$, one needs to evaluate only one of them. Using $e^{i\pi S^{y}_{i}} = S^{+}_{i} - S^{-}_{i}$, LRS for the y-component can be expressed as:

$$O^{x,y}_{l,m} = \left\langle (S^{+(b)}_{l} - S^{-(b)}_{l})(S^{+(a)}_{l+1} - S^{-(a)}_{l+1}) \ldots (S^{+(a)}_{m} - S^{-(a)}_{m}) \right\rangle . \tag{23}$$

By the use of JWT, we convert LRS for spins to fermionic LRS :

$$O^{z}_{l,m} = \left\langle e^{i\pi(b^{\dagger}_{l} b_{l} + a^{\dagger}_{l+1} a_{l+1} + \cdots + a^{\dagger}_{m} a_{m})} \right\rangle \tag{24}$$

which is obtained using the fact that the number of operators in the exponent is always even. For the transverse LRS we obtain,

$$O^{x,y}_{l,m} = \left\langle (b^{\dagger}_{l} + b_{l})(a^{\dagger}_{l+1} - a_{l+1}) \ldots (a^{\dagger}_{m} - a_{m}) \right\rangle . \tag{25}$$

We introduce the following operators for a more convenient notation:

$$A_m = (a^{\dagger}_{m} - a_{m}) \tag{26}$$

$$B_m = (a^{\dagger}_{m} + a_{m}) \tag{27}$$

$$C_m = (b^{\dagger}_{m} - b_{m}) \tag{28}$$

$$D_m = (b^{\dagger}_{m} + b_{m}). \tag{29}$$

It is straightforward to derive anticommutation relations of the pairs for introduced operators:

$$\{A_m, A_n\} = \{C_m, C_n\} = -2\delta_{m,n} \tag{30}$$

$$\{B_m, B_n\} = \{D_m, D_n\} = 2\delta_{m,n} \tag{31}$$

where $\delta_{m,n}$ is Kronecker delta function. While for any other pair N and M from the set above, we have:

$$\{M_m, N_n\} = 0. \tag{32}$$

Then, fermionized LRSs (24) and (25) can be expressed in terms of the introduced $A - B - C - D$ operators,

$$O^{z}_{l,m} = \langle D_l C_l B_{l+1} A_{l+1} \ldots D_{m-1} C_{m-1} B_m A_m \rangle \tag{33}$$

$$O^{x,y}_{l,m} = \langle D_l A_{l+1} D_{l+2} A_{l+2} \ldots A_m \rangle . \tag{34}$$

Using Wick theorem, including only non-zero contractions, we get the following result:

$$O^{z}_{1,m} = \det(K) \tag{35}$$

$$O^{x,y}_{1,m} = \det(Q) \tag{36}$$

where by site $l = 1$ we mean any chosen b site as reference and m any chosen site a which follows b. Matrix elements $K_{l,m}$ and $Q_{l,m}$ are defined as,

$$K_{l,m} = \frac{1}{2\pi} \int_{0}^{2\pi} \frac{e^{-ik(m-l)}(e^{-2ik}\cos(\theta) + \sin(\theta))}{\sqrt{1 + \sin(2\theta)\cos(2k)}} dk \tag{37}$$

$$Q_{l,m} = \frac{1}{2\pi} \int_{0}^{2\pi} \frac{e^{-ik(m-l)}(e^{-ik}\cos(\theta) + \sin(\theta))}{\sqrt{1 + \sin(2\theta)\cos(k)}} dk. \tag{38}$$

Matrices K and Q are $(m-1) \times (m-1)$ Toeplitz matrices, with their corresponding generating functions.

Finally, $O^{S(x,y,z)}$ can be evaluated as the determinant of the Toeplitz matrices in the long range limit,

$$O^{S(z)} = \lim_{m \to \infty} |\det(K)| \tag{39}$$

$$O^{S(x,y)} = \lim_{m \to \infty} |\det(Q)|. \tag{40}$$

To evaluate SOP $O^{S(\gamma)}$ analytically, one may use Szegö theorem [36] in the Haldane phase region of the phase diagram. However, on the other insulating limit this theorem is not applicable, due to the emerging zeros in the corresponding generating functions.

It can be easily seen that SOPs are unity when the wavefunction is the tensor product of maximally entangled pairs between the unit cells ($b - a$ pair), i.e.

$$|\Psi\rangle = \prod_{i=1}^{N_c - 1} \frac{(|\uparrow^{b}_{i} \downarrow^{a}_{i+1}\rangle \pm |\downarrow^{b}_{i} \uparrow^{a}_{i+1}\rangle)}{\sqrt{2}}. \tag{41}$$

This corresponds to the Haldane phase edge limit, i.e. $\cot(\theta) = 0$. In this limit, free edge spins can be observed in a chain with open boundary conditions as shown in figure 2, similar to the edge states of the $S = 1$ Heisenberg model. However, when the value of the intracell hopping is increased,

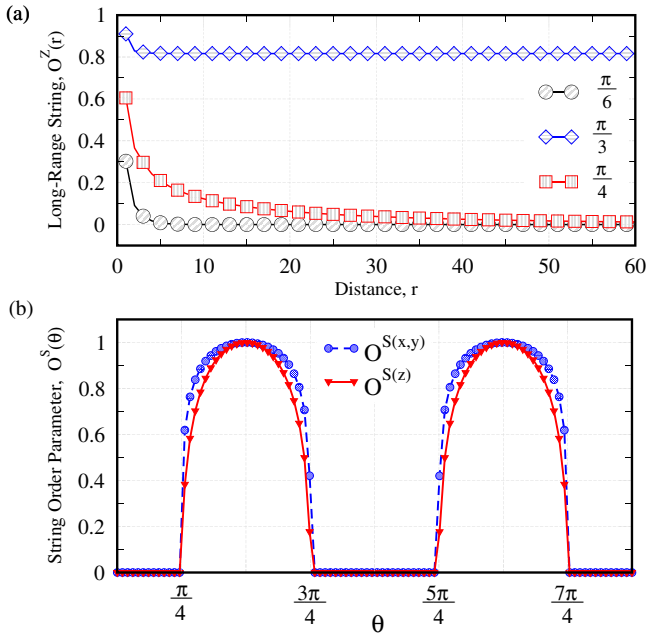

Figure 3. In (a) LRS $O^z(r)$ evaluated in the Haldane phase ($\theta = \frac{\pi}{3}$), in the trivial insulating phase ($\theta = \frac{\pi}{6}$) and in the QCP ($\theta = \frac{\pi}{4}$) are presented. SOPs $O^{S(x,y,z)}$ are evaluated as a long-distant behaviour of LRSs and shown in (b). A region of the unit circle with a finite value of $O^{S(x,z)}$ define the Haldane phase region, which is consistent with the phase diagram represented in figure 1(c).

maximally entangled spin dimers become less entangled, which results in a decreased value of $O^{S(\gamma)}$. Indeed, using Szegö theorem one can show that the value of $O^{S(z)}$ for infinitesimal intracell hopping,

$$O^{S(z)} \approx \mathrm{e}^{-\frac{\cot(\theta)^2}{4}}, (\cot(\theta) \to 0). \tag{42}$$

This result shows that for non-zero intracell hopping, $O^{S(z)}$ decreases from unity. The same behaviour can be found for $O^{S(x,y)}$. Thus, $O^{S(\gamma)}$ can be connected to the entanglement measure of $b - a$ spin pairs .

In figure 3 we plot the longitudinal LRS $O^z(r)$ for $\theta \in [\frac{\pi}{6}, \frac{\pi}{4}, \frac{\pi}{3}]$ and corresponding SOPs $O^{S(x,z)}$ within the unit circle using equations (35)–(40). Figure 3(a) shows that $O^z(r)$ exponentially converges to the finite value $O^{S(z)} \approx 0.8$ in the Haldane phase at $\theta = \frac{\pi}{3}$, while exponential convergence to $O^{S(z)} = 0$ can be observed in the trivial phase, i.e. at $\theta = \frac{\pi}{6}$. In the vicinity of quantum critical points (QCP), $O^{S(z)}(r)$ decreases accroding to a power law, which leads to the divergence of correlation length ζ at the QCP. Thus, one needs to evaluate $O^z(r)$ in the very large distance at these points to extract the value of $O^{S(z)}$. A similar behaviour can be observed on the corresponding phases for $O^{x,y}(r)$. We found the corresponding power law decrement of SOPs at the QCP to be $O^{S(z)}(r) \approx r^{-0.3}$. This is in a good agreement with bosonization result presented in [9], while the result there is presented for a dimerized isotropic Heisenberg model. Furthermore, we note that the obtained results are consistent with a superior accuracy with the result of DMRG calculations presented in [39].

In figure 3(b) we show the phase diagram of the model based on the O^S. It demonstrates that for the values of $|\cot(\theta)| < 1$, the system is in the Haldane phase, which is characterized by the finite value of SOPs. The maximum values of O^S at $\cot(\theta) = 0$. In the QCPs O^S vanish and for the remained circle sectors, i.e. $|\tan(\theta)| < 1$ the system is in the trivial phase. In analogy to (21), one may consider the following relation for LRS,

$$O^{\gamma(c)}_{l,m} = -4 \left\langle S^{\gamma(a)}_l \mathrm{e}^{\mathrm{i}\pi(S^{\gamma(b)}_{l+1} + S^{\gamma(a)}_{l+2} + \cdots + S^{\gamma(a)}_{m-1})} S^{\gamma(b)}_m \right\rangle. \tag{43}$$

In contrast to the introduced SOPs, new SOPs derived from equation (43), detect trivial phase of the model, i.e. they are unity when the maximally entangled pairs are $a - b$ spin pairs.

It should be noted that SOPs are not robust against any symmetry-breaking terms. As an example, an applied magnetic field in z direction which breaks $SU(2)$ symmetry, makes $O^{x,y}_{l,m}$ converge to a finite value even in the trivial insulating phase. An alternative example is the interacting limit, i.e. bond-alternating XXZ chain, for which SOP is a valid order parameter only for the $SU(2)$ symmetric case, i.e. in the XXX limit.

4. Entanglement and correlations

More information about the tQPT discussed in the previous section, can be extracted from a measure of local entanglement. To gain an insight about the entanglement structure of the model, we calculate the two-site density matrix and use two-site concurrence $C^{a,b}_{i,j}$ as an entanglement measure [23]. In trivial QPTs, non-analytic divergent character of the concurrence usually corresponds to first order quantum phase transitions (1QPT), while this behaviour in the derivative of the concurrence is peculiar to the second order transitions (2QPT). Thus, it is interesting to refer to which class of the trivial QPTs the tQPT corresponds. Here, we will exactly evaluate $C^{a,b}_{i,j}$ in terms of two-point correlation functions and investigate the behaviour of it and $\frac{\mathrm{d}C^{a,b}_{i,j}}{\mathrm{d}\theta}$ in QCPs.

The functional dependence of the two-site concurrence on standard correlation functions in generalized quantum spin chains was derived earlier [24] from the reduced density matrix for any two given sites of the chain. Here, we simplify this derivation using symmetries of the Hamiltonian (3).

The reduced density matrix for any given two sites i and j can be expressed in terms of two-point correlation functions in the following manner (in $|\uparrow\uparrow\rangle, |\uparrow\downarrow\rangle, |\downarrow\uparrow\rangle, |\downarrow\downarrow\rangle$ basis):

$$\rho^{(a,b)}_{i,j} = \begin{bmatrix} u^{(a,b)}_{i,j} & 0 & 0 & 0 \\ 0 & w^{(a,b)}_{i,j} & t^{(a,b)}_{i,j} & 0 \\ 0 & t^{(a,b)}_{i,j} & w^{(a,b)}_{i,j} & 0 \\ 0 & 0 & 0 & u^{(a,b)}_{i,j} \end{bmatrix} \tag{44}$$

where $u^{(a,b)}_{i,j} = \frac{1}{4} + G^{zz(a,b)}_{i,j}$, $w^{(a,b)}_{i,j} = \frac{1}{4} - G^{zz(a,b)}_{i,j}$ and $t^{(a,b)}_{i,j} = 2G^{xx(a,b)}_{i,j}$. Derivation of two-point correlation functions $G^{\gamma\gamma(a,b)}_{i,j}$ for all spin components can be found in appendix.

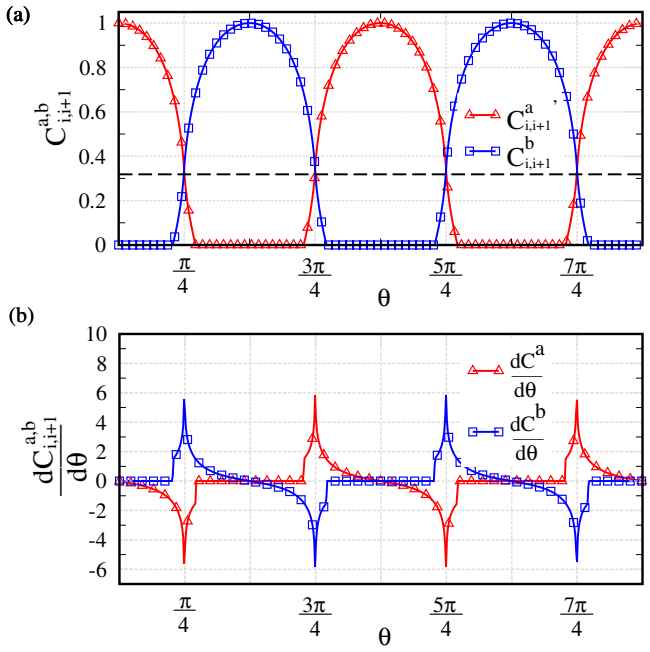

Figure 4. Calculated pairwise concurrence values for nearest neighbour $a-b$ spin pairs $C^{a}_{i,i+1}$ and nearest neighbour $b-a$ spin pairs $C^{b}_{i,i+1}$ are shown in (a). We note that for the maximally entangled spin pairs $C^{a,b}_{i,i+1}=1$, while decreasing to $C^{a}_{i,i+1}=C^{b}_{i,i+1}\approx 0.35$ (dashed line) at QCP. In these QCPs non-analytic divergent character of the $\frac{dC^{a,b}}{d\theta}$ can be noticed (b). The points of *sudden death and birth of entanglement* can be noticed with step like jumps in $\frac{dC^{a,b}}{d\theta}$.

To derive (44) we exploited the spin-flip symmetry (which leads to $\langle S^z\rangle=0$) and also the symmetry of Hamiltonian (3) with respect to the rotation in the $x-y$ plane. Due to broken inversion symmetry, one has two inequivalent $\rho^{a,b}_{i,j}$.

The concurrence of two sites $C_{i,j}$ may be computed from the density matrix $\rho_{i,j}$ as $C_{i,j}=[\lambda_1-\lambda_2-\lambda_3-\lambda_4]$, where the λ_i are the eigenvalues in decreasing order of the matrix $R=\sqrt{\sqrt{\rho}\tilde{\rho}\sqrt{\rho}}$. The matrix $\tilde{\rho}_{i,j}$ can be expressed as $\tilde{\rho}_{i,j}=(\sigma^y\otimes\sigma^y)\rho^{*}_{i,j}(\sigma^y\otimes\sigma^y)$. Then, the two site concurrence for any given sites i and j $C^{a,b}_{i,j}$ can be expressed in terms of two-point correlation functions as:

$$C^{a,b}_{i,j}=2\max\left\{0,2|G^{xx(a,b)}_{i,j}|-|\frac{1}{4}+G^{zz(a,b)}_{i,j}|\right\}. \quad (45)$$

In figure 4 we present concurrence $C^{a}_{i,i+1}$ and $C^{b}_{i,i+1}$ for nearest-neighbours calculated from equation (45). For vanishing intracell couplings (i.e. at $\theta=\frac{(2n+1)\pi}{2}, n\in\mathbb{Z}$), $C^{b}_{i,i+1}=1$, showing maximal entanglement of the $b-a$ spin pairs. This result is consistent to our SOP result corresponding to maximally entangled $b-a$ spin pairs. Non-zero intracell spin couplings, perturb this entanglement structure of pairs, inducing a decrease in $C^{b}_{i,i+1}$. This corresponds to the breaking of *entanglement monogamy* of $b-a$ spin pairs. Further decrease of $C^{b}_{i,i+1}$ continues when the intracell coupling is incremented. However, unlike the SOPs, it does not vanish at QCPs. In these gapless Luttinger liquid points every site is entangled with the nearest neighbour with the same concurrence $C^{a}_{i,i+1}=C^{b}_{i,i+1}\approx 0.35$ (marked with a dashed line). Further increment of J results in the sudden death of entanglement which happens at $\theta\approx\frac{(2n+1)\pi}{2}+\frac{50\pi}{171}, n\in\mathbb{Z}$.

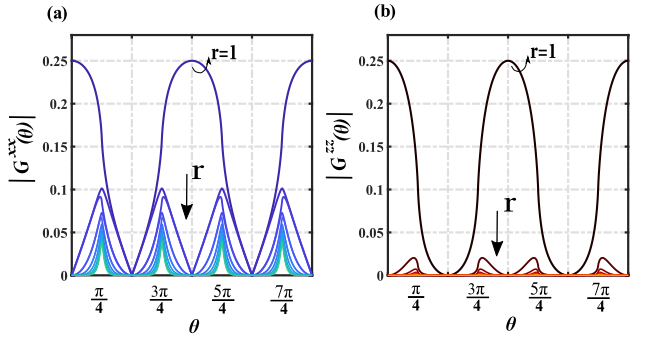

Figure 5. Modulus of two-point correlation functions $|G^{(a)xx}(\theta)|$ and $|G^{(a)zz}(\theta)|$ of $a-r$ spin pairs are shown in (a) and (b), respectively. For nearest neighbours ($r=1$) the maximum values of absolute correlations are reached in vanishing intercell couplings $J'=0$. For the next nearest neighbours ($r>1$) the maximum values are located at QCPs. Correlation functions $|G^{(a)zz}(\theta)|$ vanish for any $a-a$ spin pairs, i.e. for even r.

In the opposite way $C^{a}_{i,i+1}$ behaves, which measures an entanglement of $a-b$ spin pairs. Obviously, it is unity for vanishing intercell hopping values J.

As pointed out, the derivative of the concurrence should diverge for QCPs, at least this is what one expects in trivial QPTs. Indeed, from figure 4(b) it is clear that for $\theta=\frac{(2n+1)\pi}{4}, n\in\mathbb{Z}$, one has sharp peaks in $\frac{dC^{a,b}}{d\theta}$ signalling about the tQPT. This character is inherent for the trivial 2QPTs. Similarly, one can show that the second derivative of the ground state energy $\frac{d^2E}{d\theta^2}$ (exact form of E is presented in appendix) is also singular at QCPs, which is also a peculiarity of the 2QPTs. Except for these peaks, step like drops of the function can be noticed. These does not effect the phase diagram of the model, however, it is related to the sudden death (or birth) of the entanglement.

To characterize the divergent behaviour of $\frac{dC^{a}_{i,i+1}}{d\theta}$ for nearest-neighbour $a-b$ pairs, for simplicity, we consider $\theta\in[0,\frac{\pi}{2})$. In this limit, equation (45) can be expressed as,

$$C^{a}_{i,i+1}\left(0\leqslant\theta<\frac{\pi}{2}\right)=\max\left\{0,2(W_1(\theta)-\frac{1}{2})^2-1\right\} \quad (46)$$

where $W_1(\theta)$ is defined in equation (A.9). Then, the singularity character of $\frac{dC^{a}_{i,i+1}}{d\theta}$ can be effectively described via,

$$\frac{dC^{a}_{i,i+1}}{d\theta}=4(W_1(\theta)-\frac{1}{2})\frac{dW_1(\theta)}{d\theta}. \quad (47)$$

Note, that equation (47) is valid for $(W_1(\theta)-\frac{1}{2})^2>\frac{1}{2}$, i.e. till the entanglement death point is reached. Both integrals $W_1(\theta)$ and $\frac{dW_1(\theta)}{d\theta}$ are linear combination of complete Elliptic integrals of the First ($\mathcal{K}(x)$) and the Second ($\mathcal{E}(x)$) kinds.

In the vicinity of the QCP, $\theta\to\theta_c$, $W_1(\theta)$ is continious function with $W_1(\frac{\pi}{4})=-\frac{1}{\pi}$, while $\frac{dW_1}{d\theta}\approx\frac{\mathcal{K}(\frac{2\sin(2\theta)}{1+\sin(2\theta)})-2}{\pi}$. Exploiting an asymptotic expansion in the leading order, $\mathcal{K}(1-\frac{\epsilon^2}{2})\approx-\log(\epsilon)+\frac{5}{2}\log(2)$ $(\epsilon\to 0)$, yields to the logarithmic divergence of $\frac{dC^{a}_{i,i+1}}{d\theta}$:

$$\frac{\mathrm{d}C^{a}_{i,i+1}}{\mathrm{d}\theta} = \frac{4+2\pi}{\pi^2}\log(\theta-\theta_c) + \text{const.} \tag{48}$$

Similar to the critical behaviour of the *XY* model [29], the derivative of the concurrence has a logarithmic divergence, indicating the Ising universality class of the transition.

The concurrences for next neighbours $C^{a,b}_{i,i+r} = 0$ for all values of θ. To show this and to clarify the origin of the singular peaks, in figure 5 we plot the absolute value of the two-point correlation functions $|G^{xx}(r,\theta)| = |\langle S_i^{x(a)} S_{i+r}^{x(a,b)}\rangle|$ and $|G^{zz}(r,\theta)| = |\langle S_i^{z(a)} S_{i+r}^{z(a,b)}\rangle|$ for $a-r$ pair of spins. To begin with, the derivative of nearest-neighbour correlators have singular peaks at QCP (not shown), resulting in similar peaks of the concurrence. However, derivatives of these correlators for other distances vanish at QCPs, since these points are stationary points. This can be seen from figures 5(a) and (b) where the absolute value of correlators for other distances have a maximum value at QCPs. These values decrease with distance, which is known to have a power law behaviour. One may notice that for $r > 1$, the value of $2|G^{xx}| - |1/4 + G^{zz}| < 0$. Thus, from equation (45) one concludes that $C^{a,b}_{i,i+r}$ vanish for $(r > 1)$, i.e. starting from the next nearest neighbours.

In contrast to the derived SOPs, the two-site concurrences are universal: they identify diverse types of quantum phase transitions even in the presence of symmetry-breaking terms. In this respect, SOPs are limited on application, one should modify them in a necessary way to determine the phase transition. For this, of course, one needs to have a priliminary knowledge of the corresponding phases. On the other hand, the two-site concurrence similar to the other quantum information tools to study QPTs, does not clarify the nature of transitions. Since it captures trivial and topological QPTs equivalently in the same manner, there is no way to distinguish phases of the transition. This again opens the question of classification of phases, which can be particularly performed by non-local order parameters such as SOPs.

5. Summary and conclusions

In this paper, we discussed the implementation algorithm of string order parameter (SOP) as an exactly calculable order parameter for the symmetry-protected topological phase (SPT) phases and studied the local pairwise entanglement behaviour at topological quantum phase transition (tQPT). We mapped the bond-alternating spin chain via Jordan–Wigner fermionization to the generalized version of the SSH model and demonstrated the correspondence of the topological insulating phase of the standard SSH model and the Haldane phase of the bond-alternating spin model. We derived exact analytical expressions for two-point transverse and longitudinal correlation functions. By the fermionization of the longitudinal and transverse SOPs we showed the exact expression of them in terms of the determinant of the Toeplitz matrices with the given generating functions. We demonstrated that the derived expressions of SOPs take their maximal value of unity in the fully dimerized SPT Haldane phase and vanish in the trivial insulating phase. To get more insight about the phase transition, we studied pairwise local entanglement (namely, two-site concurrence) in the vicinity of tQPTs. We found that the two-site concurrence vanishes for all other distances except the nearest neighbour, like in the standard Heisenberg model. The derivative of the concurrence has a singularity at the tQPT, like in trivial second order quantum phase transitions. In contrast to the SOPs, we found the two-site concurrence robust against symmetry-breaking terms and its application as an additional order parameter to be practical.

For future outlook, we note that our result of fermionized SOPs can be extended for other 1D spin chains and ladder models. However, the more important topic of fragility of SOPs needs to be investigated in a more detailed way, considering symmetries of the models.

Acknowledgments

MSB thanks Prof Aikaterini Mandilara for useful discussions and acknowledges ORAU grant “Dissecting the collective dynamics of arrays of superconducting circuits and quantum metamaterials” (no. SST2017031) for the support of his short stay in Nazarbayev University.

MSB and JS thank the Deutsche Forschungsgemeinschaft DFG (355031190 (FOR 2692); 397300368 (SCHN 615/25-1)) for generous support.

Appendix. Calculation of zero-temperature correlation functions

To evaluate the ground state energy per spin, one needs to integrate the band below the Fermi energy, which leads to:

$$\epsilon_G = \frac{E_G}{N} = -\frac{|\cos(\theta)+\sin(\theta)|}{\pi}\mathcal{E}\left(\frac{2\sin(2\theta)}{1+\sin(2\theta)}\right) \tag{A.1}$$

where $\mathcal{E}(x)$ is the Elliptic integral of the Second kind. To evaluate static two-point correlator as the function of spin couplings, we rewrite creation and annihilation operators in terms of quasiparticle operators:

$$a_q = \frac{1}{\sqrt{2}\mathrm{A}_q}(\beta_q - \alpha_q) \tag{A.2}$$

$$b_q = \frac{1}{\sqrt{2}}(\alpha_q + \beta_q). \tag{A.3}$$

From the definition of quasiparticle vacuum one can get following relationships:

$$\left\langle b_k^{\dagger} a_q \right\rangle = -\frac{\delta_{q,k}}{2A_k} \tag{A.4}$$

$$\left\langle a_k^{\dagger} b_q \right\rangle = -\frac{\delta_{q,k}}{2A_k^*} \tag{A.5}$$

where

$$A_k = \frac{E^+(2k)}{\mathrm{e}^{\mathrm{i}k}\sin(\theta) + \mathrm{e}^{-\mathrm{i}k}\cos(\theta)}. \tag{A.6}$$

One can show that,

$$\left\langle a_k^\dagger a_q \right\rangle = \left\langle b_k^\dagger b_q \right\rangle = \frac{\delta_{q,k}}{2}. \tag{A.7}$$

Using anticommutation relations one can get a remained matrix elements. Obviously, for even $r = n - m$ correlation functions $\langle a_m^\dagger a_n \rangle = \langle b_m^\dagger b_n \rangle$ vanish:

$$\left\langle a_m^\dagger a_n \right\rangle = \left\langle b_m^\dagger b_n \right\rangle = \frac{\sin\left(\frac{\pi(n-m)}{2}\right)}{\pi(n-m)} = 0. \tag{A.8}$$

Here, indexes do not correspond to the effective unit cell, but to a site, thus we will work in a *reduced Brillouin zone*.

Next, we evaluate non-vanishing correlation functions $W_{n-m} = \langle a_m^\dagger b_n \rangle$ and $Z_{n-m} = \langle b_m^\dagger a_n \rangle$; Further, we assume $n > m$.

$$W_{n-m} = -\frac{1}{2\pi} \int_{-\frac{\pi}{2}}^{\frac{\pi}{2}} \frac{\mathrm{e}^{-\mathrm{i}kr}(\mathrm{e}^{\mathrm{i}k}\cos(\theta) + \mathrm{e}^{-\mathrm{i}k}\sin(\theta))}{\sqrt{1+\sin(2\theta)\cos(2k)}}\mathrm{d}k. \tag{A.9}$$

Another non-vanishing correlator is:

$$Z_{n-m} = -\frac{1}{2\pi} \int_{-\frac{\pi}{2}}^{\frac{\pi}{2}} \frac{\mathrm{e}^{-\mathrm{i}kr}(\mathrm{e}^{\mathrm{i}k}\sin(\theta) + \mathrm{e}^{-\mathrm{i}k}\cos(\theta))}{\sqrt{1+\sin(2\theta)\cos(2k)}}\mathrm{d}k. \tag{A.10}$$

It is can be noticed that $W_r = Z_{-r}$. Integrals above for nearest neighbours (i.e. $|r| = 1$) are the linear composition of $K(\sin(\theta), \cos(\theta))$ and $E(\sin(\theta), \cos(\theta))$ which are elliptic integrals of the first and the second kinds. For remaining distances, the analytical solution is involved and the integration consists other terms.

A.1. Transverse correlation functions

We consider correlation function of x—components of spins, i.e. $G_{m,n}^{xx(a)} = \langle S_m^{(a)x} S_n^{(b)x} \rangle$

$$G_{m,n}^{xx(a)} = \frac{1}{4}\left\langle (S_m^{(a)+} + S_m^{(a)-})(S_n^{(b)+} + S_n^{(b)-}) \right\rangle. \tag{A.11}$$

Index a in $G_{m,n}^{xx(a)}$ shows that we look x-component correlation of any $a - b$ spin pair. In fermionic representation it has the following form:

$$G_{m,n}^{xx(a)} = \frac{1}{4}\left\langle (a_m^\dagger - a_m)\mathrm{e}^{\mathrm{i}\pi\sum_{k=m+1}^{k=n-1}(\hat{n}_k^{(a,b)})}(b_n^\dagger + b_n) \right\rangle. \tag{A.12}$$

Thus, we have for every site one has exponential string operator:

$$\mathrm{e}^{\mathrm{i}\pi p_k^\dagger p_k} = (1 - 2p_k^\dagger p_k) = (p_k^\dagger + p_k)(p_k^\dagger - p_k) \tag{A.13}$$

where $p = a, b$ is fermionic operator. Equation (A.12) can be written in terms of $A - B - C - D$ operators (26)–(29) as:

$$G_{m,n}^{xx(a)} = \frac{1}{4}\left\langle A_m D_{m+1} C_{m+1} B_{m+2} A_{m+2} \ldots B_{n-1} A_{n-1} D_n \right\rangle. \tag{A.14}$$

One can evaluate this correlation function using Wick theorem, since operators anticommute. Thus, we firstly evaluate expectation values of the form $\langle N_m M_n \rangle$ where N and M belong to a set of operators defined in (26)–(29).

Using (A.8) it can be shown that for different sites $\langle N_m N_n \rangle = 0$ for any N. Furthermore, $\langle A_m B_n \rangle = \langle C_m D_n \rangle = 0$.

The only non-zero elements are:

$$\langle A_m D_n \rangle = 2W_{n-m} \tag{A.15}$$

$$\langle C_m B_n \rangle = 2Z_{n-m}. \tag{A.16}$$

At this point, this information is enough to evaluate expression (A.11) using Wick theorem which leads to the following results:

$$G_{1,n}^{xx(a)} = \frac{1}{4}\det\begin{bmatrix} 2W_1 & 0 & 2W_3 & 0 & \ldots & 2W_{n-1} \\ 0 & 2Z_1 & 0 & 2Z_3 & \ldots & 0 \\ 2W_{-1} & 0 & 2W_1 & 0 & \ldots & 2W_{n-3} \\ 0 & 2Z_{-1} & 0 & 2Z_1 & \ddots & 0 \\ \ldots & \ldots & \ldots & \ldots & \ldots & \ldots \end{bmatrix} \tag{A.17}$$

where matrix elements of G^{xx} are defined by W_{n-m} and Z_{n-m}. While for the standard XY model [37, 38] the matrix G^{xx} is a well studied Toeplitz matrix, in our case the matrix is a block Toeplitz matrix, where diagonal elements oscillate between two values.

We note that using (A.17) $G^{xx(a)}$ can be evaluated for any $a - x$ pair, where $x \in [a, b]$. Obviously, $G_{m,n}^{xx(b)} \neq G_{m,n}^{xx(a)}$. It is straightforward task to show that an equivalent matrix for $G_{m,n}^{xx(b)}$ can be obtained by changing $W_{n-m} \to Z_{n-m}$.

Finally, we note that due to the isotropy of the model in $x - y$ plane, the the correlation function for y—component behaves in the same way.

A.2. Longitudinal correlation function

Calculation of $G_{m,n}^{zz}$ is not as complex job as transverse correlation functions. We firstly consider $\left\langle S_m^{(a)z} S_n^{(b(z)} \right\rangle$ case, longitudinal correlation of $a - b$ spin pairs:

$$G_{m,n}^{zz(a)} = \left\langle S_m^{(a)z} S_n^{(b)z} \right\rangle = -\frac{1}{4}\left\langle \mathrm{e}^{\mathrm{i}\pi S_m^{(a)z}} \mathrm{e}^{\mathrm{i}\pi S_n^{(b)z}} \right\rangle. \tag{A.18}$$

Fermionized expression is,

$$G_{m,n}^{zz(a)} = -\frac{1}{4}\left\langle \mathrm{e}^{\mathrm{i}\pi a_m^\dagger a_m} \mathrm{e}^{\mathrm{i}\pi b_n^\dagger b_n} \right\rangle. \tag{A.19}$$

In terms of $A - B - C - D$ operators,

$$G_{m,n}^{zz(a)} = -\frac{1}{4}\left\langle B_m A_m D_n C_n \right\rangle. \tag{A.20}$$

The only non-zero contraction is:

$$\left\langle B_m C_n \right\rangle \left\langle D_n A_m \right\rangle. \tag{A.21}$$

Thus,

$$G_{m,n}^{zz(a)} = \frac{1}{4}\left\langle B_m C_n \right\rangle \left\langle D_n A_m \right\rangle = -(W_{n-m})^2. \tag{A.22}$$

Similarly, an expression for a longitudinal correlation function of $b - a$ spin pairs is,

$$G_{m,n}^{zz(b)} = \left\langle S_m^{(b)z} S_n^{(a)z} \right\rangle = -(Z_{n-m})^2. \tag{A.23}$$

For even distances ($a - a$ spin pair or $b - b$ spin pairs), $C_{m,n}^{zz(a,b)}$ vanishes, due to the fact that all contractions of the same type of fermions (i.e. consisting only a's or b's) vanish in any permutations.

Finally, we note that analytically obtained resuts of phase diagram, SOPs and ground state properties are consistent with numerically performed DMRG studies, which are presented in [39].

ORCID iDs

Murod S Bahovadinov https://orcid.org/0000-0001-7237-3226

References

[1] Haldane F D M 1983 *Phys. Lett.* A **93** 464
[2] Haldane F D M 1983 *Phys. Rev. Lett.* **50** 1153
[3] Affleck I, Kennedy T, Lieb E H and Tasaki H 1988 *Condensed Matter Physics and Exactly Soluble Models* (New York: Springer) pp 253–304
[4] den Nijs M and Rommelse K 1989 *Phys. Rev.* B **40** 4709
[5] Kennedy T and Tasaki H 1992 *Phys. Rev.* B **45** 304
[6] Hida K 1991 *J. Phys. Soc. Japan* **60** 1347
[7] Kennedy T 1990 *J. Phys.: Condens. Matter* **2** 5737
[8] Hida K 1992 *Phys. Rev.* B **45** 2207
[9] Hida K 1992 *Phys. Rev.* B **46** 8268
[10] Hirano T, Katsura H and Hatsugai Y 2008 *Phys. Rev.* B **77** 094431
[11] Maruyama I, Hirano T and Hatsugai Y 2009 *Phys. Rev.* B **79** 115107
[12] Anfuso F and Rosch A 2007 *Phys. Rev.* B **75** 144420
[13] Anfuso F and Rosch A 2007 *Phys. Rev.* B **76** 085124
[14] Catuneanu A., Sørensen E.S. and Kee H.Y. 2019 Nonlocal string order parameter in the S = 1/2 Kitaev-Heisenberg ladder *Phys. Rev.* B **99** 195112
[15] Xu J, Gu Q and Mueller E J 2018 *Phys. Rev. Lett.* **120** 085301
[16] Lisandrini F T, Lobos A M, Dobry A O and Gazza C J 2017 *Phys. Rev.* B **96** 075124
[17] White S R 1992 *Phys. Rev. Lett.* **69** 2863
[18] Schollwöck U 2011 *Ann. Phys., NY* **326** 96
[19] Jiang H-C, Wang Z and Balents L 2012 *Nat. Phys.* **8** 902
[20] Li H and Haldane F D M 2008 *Phys. Rev. Lett.* **101** 010504
[21] Pollmann F, Turner A M, Berg E and Oshikawa M 2010 *Phys. Rev.* B **81** 064439
[22] Nehra R, Bhakuni D S, Gangadharaiah S and Sharma A 2018 *Phys. Rev.* B **98** 045120
[23] Wootters W K 1998 *Phys. Rev. Lett.* **80** 2245
[24] Glaser U, Büttner H and Fehske H 2003 *Phys. Rev.* A **68** 032318
[25] Dillenschneider R 2008 *Phys. Rev.* B **78** 224413
[26] Arnesen M, Bose S and Vedral V 2001 *Phys. Rev. Lett.* **87** 017901
[27] Osborne T J and Nielsen M A 2002 *Phys. Rev.* A **66** 032110
[28] Vidal G, Latorre J I, Rico E and Kitaev A 2003 *Phys. Rev. Lett.* **90** 227902
[29] Osterloh A, Amico L, Falci G and Fazio R 2002 *Nature* **416** 608
[30] Wu L-A, Sarandy M S and Lidar D A 2004 *Phys. Rev. Lett.* **93** 250404
[31] Jordan P and Wigner E P 1928 *Z. Phys.* **47** 631
[32] Su W-P, Schrieffer J and Heeger A 1980 *Phys. Rev.* B **22** 2099
[33] Asbóth J K, Oroszlány L and Pályi A 2016 *A Short Course on Topological Insulators* (New York: Springer) pp 1–22
[34] Wang H T, Li B and Cho S Y 2013 *Phys. Rev.* B **87** 054402
[35] Haghshenas R, Langari A and Rezakhani A 2014 *J. Phys.: Condens. Matter* **26** 456001
[36] Szegö G 1915 *Math. Ann.* **76** 490
[37] Lieb E, Schultz T and Mattis D 1961 *Ann. Phys., NY* **16** 407
[38] McCoy B M and Wu T T 1967 *Phys. Rev.* **162** 436
[39] Bahovadinov M 2019 Haldane phase in the bond-alternating spin-1/2 *XXZ* chain: DMRG, fermionization studies *Master's Thesis* Bilkent University, Ankara and Turkey